Eur Biophys J (2004) 33: 715–725
DOI 10.1007/s00249-004-0417-0

ARTICLE

Zoran Arsov · Milan Schara · Matjaž Zorko
Janez Štrancar

The membrane lateral domain approach in the studies of lipid–protein interaction of GPI-anchored bovine erythrocyte acetylcholinesterase

Received: 14 October 2003 / Revised: 20 April 2004 / Accepted: 3 May 2004 / Published online: 6 July 2004

Abstract A novel membrane lateral domain approach was used to test whether the activity of the membrane-bound enzyme acetylcholinesterase (AChE) depends on the local properties (e.g. local lipid ordering) of bovine erythrocyte-ghost membrane. This issue has an additional aspect of interest due to an alternative mode of insertion of AChE molecules into the membrane by the glycosylphosphatidylinositol (GPI) anchor. In our experiments the lateral domain membrane structure was influenced by temperature and by the addition of *n*-butanol, and was quantitatively characterized using the method of EPR spectrum decomposition. The activity of AChE was determined by a colorimetric assay in the same samples. The results show that the membrane stabilizes the conformation of the membrane-bound AChE compared to the isolated AChE. In addition, a correlation was observed between the temperature dependence of order parameter of the most-ordered domain type and the activity of AChE. Therefore, our findings support the idea that the function of GPI proteins can be modulated by the lipid bilayer. Based on the assumption that the overall activity of AChE depends on the order parameters of particular domain types as well as their proportions, two models for AChE activity were introduced. In the first, a random distribution of enzyme molecules was proposed, and in the second, localization of enzyme molecules in a single (cholesterol-rich) domain type was assumed. Better agreement between measured and calculated activity values speaks in favor of the second model.

Z. Arsov (✉) · M. Schara · J. Štrancar
Laboratory of Biophysics, Jožef Stefan Institute,
Jamova 39, 1000 Ljubljana, Slovenia
E-mail: zoran.arsov@ijs.si
Tel.: +386-1-4773648
Fax: +386-1-4263269

M. Zorko
Institute of Biochemistry, Medical Faculty,
University of Ljubljana, Vrazov trg 2,
1000 Ljubljana, Slovenia

Keywords Lateral lipid domains · EPR spectroscopy · GPI-anchored proteins · Lipid–protein interaction · Arrhenius plot

Abbreviations AChE: Acetylcholinesterase · ATCI: Acetylthiocholine iodide · DTNB: 5,5′-Dithio-bis(2-nitrobenzoic acid) · EPR: Electron paramagnetic resonance · GPI: Glycosylphosphatidylinositol · PBS: Phosphate buffer saline

Introduction

Membrane fluidity reflects the ordering and dynamics of the phospholipid acyl chains in the membrane's bilayer. The ordering is described with order parameter *S*, which represents the time-averaged angular fluctuation of the acyl-chain segments from the normal to the bilayer plane (Hubbell and McConnell 1971), and the dynamics are described with rotational correlation time, which indicates the average time required for the molecular segments to forget their previous orientation (Freed 1976). The fluidity can be altered by external influences such as changes in temperature or by the addition of compounds that interact with the membrane. Because the fluidity of the lipid environment can have an effect on the function of membrane-bound proteins (Shinitzky 1984), the basic step in the study of lipid–protein interaction is to find the correlation between dependence of membrane fluidity on the external influences and the relationships to protein function (Gordon et al. 1980; Ogiso et al. 1981; Davis and Poznansky 1987; Squier et al. 1988; Mitchell et al. 1996).

Recently, with the upgrade to the heterogeneous picture of membrane structure (Welti and Glaser 1994; Edidin 1997), it is thought more and more that lipid–protein interaction should be studied in view of bilayer lateral heterogeneity (Tocanne et al. 1994; Marsh 1995; Hønger et al. 1996; Yang and Glaser 1996). There-

fore, it seems appropriate to use the membrane lateral domain approach in the study of lipid–protein interaction, where the correlation between the local membrane ordering in the particular domain (instead of the mean membrane ordering) and protein function is sought.

The membrane lateral heterogeneity is reflected in the presence of lateral lipid domains (Fig. 1). A lateral lipid domain is usually considered to be a spatially limited region of a membrane distinguished from its neighboring regions by one or more measurable properties (Bloom and Thewalt 1995), e.g. molecular ordering and dynamics. A group of domains with similar properties represents a particular domain type. Spin-label electron paramagnetic resonance (EPR) allows us to characterize the membrane fluidity (Marsh 1981). In addition, EPR with its characteristic motional time scale averaging 10^{-8} s (defined by the spin probe's nitroxide spin Hamiltonian interaction tensor anisotropy) is appropriate for examining the lateral heterogeneous structure of membranes, because the lateral diffusion of the spin probe's molecules is too slow to average out the differences between the domains. On the other hand, under physiological conditions, the rotational motion of molecules is fast. Accordingly, we believe that the fast-motion approximation allows a sufficiently reasonable description of the spectra of fatty acid-derived spin probes in fluid biological membranes (at physiological temperatures). The observed lateral membrane domains are long-lived in comparison to the above-defined time scale. Consequently, the heterogeneity of a cell membrane (Fig. 1) results in a spectrum that is a superimposition of several spectral components corresponding to particular domain types (Fig. 2). Therefore, the EPR spectrum decomposition and the analysis of the spectral parameters enable us to measure the local membrane fluidity characteristics, i.e. the order parameters S_i and the rotational correlation times of a particular lipid domain type i, and to measure the domain-type proportions w_i. It has to be emphasized, for simplicity, that we will not deal with the problem of the difference between the membrane structure of the exoplasmic and the cytoplasmic membrane leaflets (Devaux 1991; Žuvič-Butorac et al. 1999).

Since the membrane-bound enzyme activity may depend on the properties of a particular lipid domain type, the overall activity A can be calculated as a weighted sum of the local enzyme activities A_i in the corresponding particular domain type i

$$A = \sum_i A_i \frac{N_e^i}{N_e^{\text{total}}} \tag{1}$$

where $N_e{}^i$ is the number of enzyme molecules in domain type i, and $N_e{}^{\text{total}} = \Sigma_i\, N_e{}^i$, the total number of enzyme molecules. The domain-type activity A_i may depend on the local membrane features, e.g. on domain-type order parameter S_i. The ratio $N_e{}^i/N_e{}^{\text{total}}$ can be calculated from the proportion of a particular domain type w_i, if the partitioning of enzyme molecules between different domain types is known. Consequently, if the overall activity A is to be determined, the properties of each domain type should be characterized. Hence, the membrane lateral domain approach should be used. Such an approach might be suitable in the case of the erythrocyte membrane-bound enzyme acetylcholinesterase (AChE), because the erythrocyte membrane shows lateral heterogeneity (Rodgers and Glaser 1991; Tomishige and Kusumi 1999; Žuvič-Butorac et al. 1999; Arsov et al. 2002).

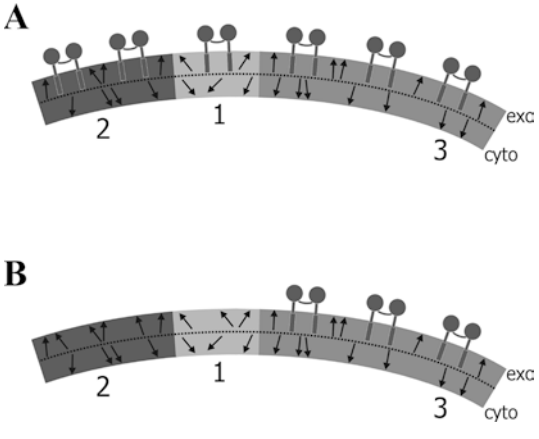

Fig. 1A, B Assumed distributions of AChE molecules in the lipid bilayer. **A** Model 1: a random distribution of enzyme molecules. **B** Model 2: enzyme molecules reside in the most-ordered domain type. The lipid bilayer (composed of *exo*- and *cyto*plasmic leaflets) is presented as composed of three lateral lipid domain populations ($i = 1, 2, 3$) in which AChE molecules in dimeric form (represented as *filled circles linked together*) and the spin probe molecules (*arrows*) are partitioned. Consequently, the EPR spectrum is decomposed to three spectral components each corresponding to a particular lipid domain population (see Fig. 2)

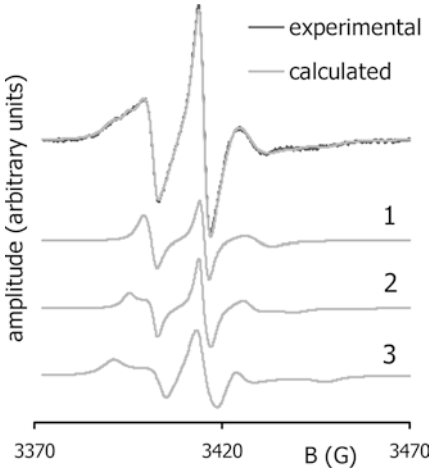

Fig. 2 Experimental EPR spectrum of the spin-labeled bovine erythrocyte-ghost membrane (concentration of *n*-butanol 0.22 M, $T = 297.5$ K) compared with the simulated spectrum. The simulated spectrum is decomposed into three spectral components ($i = 1, 2, 3$). The spectral parameters of a particular spectral component are related to the properties of a particular domain type

The issue of lipid–protein interaction in the case of AChE has an additional aspect of interest due to an alternative mode of insertion of AChE in the erythrocyte membrane by a complex glycosylphosphatidylinositol (GPI) anchor (Futerman et al. 1985). AChE is mainly in dimeric form (Taguchi and Ikezawa 1987) and positioned in the exoplasmic leaflet of the membrane (Low and Saltiel 1988). The question of modulation of AChE activity by the changed fluidity of the lipid environment has already been raised (see review by Spinedi et al. 1993). However, recent indications that the conformation of a GPI protein (and consequently its function) can be modulated by the lipid bilayer through the GPI anchor (Barboni et al. 1995; Lehto and Sharom 1998) offer new motivation to verify the dependence of the function of GPI-anchored proteins on the physical state of the hosting membrane.

In this work, we studied the dependence of the GPI-anchored AChE enzyme activity on the lateral heterogeneity of the membrane of bovine erythrocyte ghosts. The membrane lateral domain structure (characterized using EPR) and the activity of AChE were determined on the same samples of ghosts. In order to check whether the membrane affects the enzyme function, the dependence of activity of intact enzyme as well as isolated enzyme on temperature and on concentration of *n*-butanol was compared. Furthermore, we explored the relationship between the modulations of the membrane properties induced by the above stresses and the activity of intact erythrocyte AChE. Assuming that the overall activity of the membrane-bound AChE depends on the properties of different domain types and on domain-type proportions, two models for describing the AChE activity were introduced. In the first model, a random distribution of enzyme molecules in the membrane was assumed, while in the second model the localization of enzyme molecules in a single domain type was assumed (Fig. 1).

Materials and methods

Preparation of erythrocyte ghosts

The erythrocyte hematocrit was prepared by washing fresh bovine blood with a phosphate buffer saline (PBS), pH 7.4, three times. Next, 12 ml of 50% hematocrit was chilled to 0 °C and 120 ml of 4 mM $MgSO_4$ solution was added. The solution was stirred and left to mix for 5 min, all at 0 °C. After that, 7 ml of 3.32 M NaCl was added. The solution was stirred and left to mix for 5 min, all at 0 °C. The obtained mixture was incubated for approximately 50 min at 37 °C and then cooled and centrifuged at 25,000 *g* for 15 min. The centrifugation (and washing with PBS at the same time) was conducted three times. Three experiments were made and new erythrocyte ghosts were prepared each time.

Spin labeling and measurement of EPR spectra

A total of 60 µl of 10^{-4} M lipophilic spin probe, methyl ester of 5-doxyl palmitate MeFASL(10,3) in ethanol, was added to the glass tube. The ethanol was evaporated so that the spin probe was uniformly distributed over the walls of the glass tube. After the final wash, the ghosts were suspended in a volume approximately three times larger than the volume of the membrane pellet. An appropriate volume of this suspension was added to the glass tube, so that the total volume (with the *n*-butanol added) of the sample was 750 µl. The tube was then shaken for 3 min. After that the labeled sample was centrifuged at 25,000 *g* for 5 min. The pellet was transferred into quartz capillary (1-mm inner diameter) and the EPR spectra were recorded on a Bruker ESP 300 spectrometer (frequency 9.59 GHz, microwave power 20 mW). The spectra were accumulated in two to three scans (with 167 s/scan) in order to obtain a high signal-to-noise ratio. The ratio of the number of spin labels to lipid molecules was approximately 1:200.

The EPR spectra decomposition and the determination of parameters

The EPR spectra simulation and optimization were carried out according to the method presented by Arsov et al. (2002). In the following paragraphs, the method is briefly summarized.

The spectrum-simulation model was the so-called motional-restricted fast-motion approximation (Štrancar et al. 2000). Assuming the coexistence of long-lived lateral domains on the EPR timescale, we expect that each spectrum is a superimposition of the spectral components that identify the membrane heterogeneity in the sample. The properties of a particular domain type are directly reflected in the values of the chosen parameter set. The set consists of order parameter S, effective rotational correlation time, additional broadening constant, hyperfine and Zeeman tensors' polarity correction factors, and weighting factors (proportions) w.

The software (EPRSIM, version 4.9) allowed us to decompose a spectrum $I(B)$ into different predefined numbers of spectral components $I_i(B)$ (at most five) related to the domain types with different parameter sets in a magnetic field B:

$$I(B) = \sum_i I_i(B) w_i \tag{2}$$

where i is the domain-type index, and w_i is the proportion so that $\Sigma_i\, w_i = 1$. The parameters of the model were tuned by a hybrid evolutionary-optimization procedure, which combines the deterministic simplex algorithm and the stochastic genetic algorithm (Filipič and Štrancar 2001). Because two spectral components ($i = 1, 3$) were not enough to obtain a satisfactory fit according to our measurement of the goodness of fit, the predefined number of spectral components was chosen to be three

(Fig. 2). In addition, the best fit between the measured and the calculated spectra was assessed visually from a set of fits provided by multiple runs of the optimization (the optimization of each spectrum was done six times). It is worth remembering that the probability of finding the global minimum is very high due to the use of the stochastic genetic algorithm. The best-fit spectrum-simulation parameters were used to draw the plots presented in the Results.

Enzyme activity determination

The enzyme activity measurements were performed on the same pool of erythrocyte ghosts as used for the EPR measurements. The activity was determined by the Ellman method (Ellman et al. 1961). The assay mixture (3 ml) contained PBS (pH 7.4), 0.33 mM 5,5′-dithiobis(2-nitrobenzoic acid) (DTNB) and 30–120 μg of membrane protein for samples without *n*-butanol (and appropriate concentration of *n*-butanol for alcohol samples). The phosphate buffer solution was heated to the appropriate temperature before making the assay mixture. After temperature equilibration of the cuvette with the assay mixture in the thermostatically controlled cuvette holder of the spectrophotometer for 5 min, the reaction was started by the addition of an appropriate volume of substrate acetylthiocholine iodide (ATCI) to give the initial substrate concentration of 0.5 mM. The increase in the absorbance at 412 nm was monitored with a Beckman DU7500 UV/visible spectrophotometer and recorded for 120 s. The activity of the enzyme was calculated from the slope of absorbance versus time. All enzyme activity measurements were carried out in triplicate. DTNB and ACTI were purchased from Sigma Chemical (USA). The protein content was determined by the method of Lowry (Lowry et al. 1951) using bovine serum albumin as standard.

The choice of the appropriate substrate concentration and buffer (Spinedi et al. 1988) helped us to avoid the artefact breaks that might arise in Arrhenius plots (Silvius et al. 1978). In order to be able to measure the activity at high protein contents and to ignore the release of thiol material from the erythrocytes and the contribution of plasma esterases, the experiments were done on erythrocyte ghosts. For the amounts of the enzyme used, the rate of non-enzymatic hydrolysis of ATCI did not influence the obtained values of activity (its contribution was in the range of error).

In the experiments with isolated bovine erythrocyte AChE, purchased from Sigma Chemical (USA), the enzyme solution was added to the assay mixture instead of the erythrocyte ghosts. The solution of isolated AChE was prepared by dissolving 20 mg of the sample of isolated AChE in 10 ml of PBS. This solution was vortexed for 30 min and centrifuged at 1,200 *g* for 15 min. The supernatant was collected and used as a source of the isolated AChE. A total of 800 μl of this solution was added to the assay mixture.

According to the results of previous experiments (Arsov et al. 2002) we decided to use 0.22 M *n*-butanol in the assay mixture (for alcohol samples). Firstly, at this concentration, the plot of the temperature dependence of the order parameter of the most-ordered domain type shows a break. Secondly, the temperature at which the break occurs (306 K in the present experiment; see Fig. 3A) is below the temperature at which the increase in the enzyme activity diminishes (309 K, Spinedi et al. 1988; 310 K, present experiment; see Fig. 3B), and below the temperature of the start of the denaturation process (315 K, present experiment, as judged by the decrease in the enzyme activity; see Figs. 3B, 4). The above criteria are not fulfilled for other *n*-butanol concentrations (0.07, 0.15 and 0.37 M), which were also used in the previous experiment (Arsov et al. 2002).

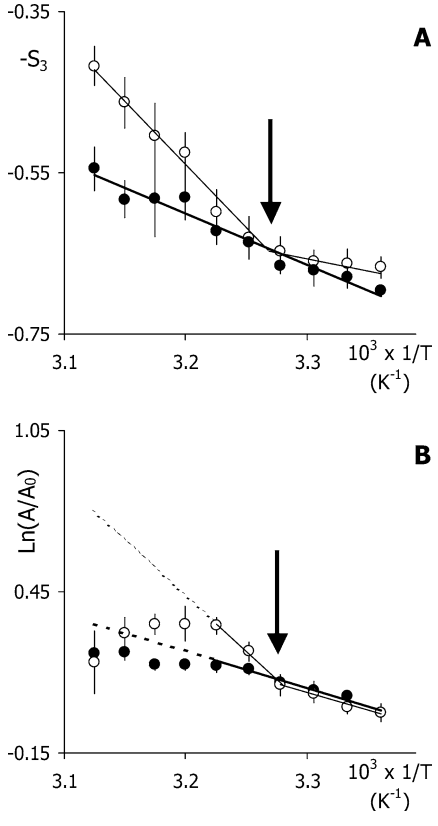

Fig. 3 The correlation of temperature dependence of **A** the order parameter of the most-ordered domain type S_3 in the erythrocyte-ghost membrane and **B** the erythrocyte AChE activity. Measured values are shown as *filled* and *open circles* for control and *n*-butanol samples (0.22 M), respectively. The activities of control and alcohol samples are normalized to their corresponding values at 297.5 K. The *dashed lines* in **B** are extrapolations of the fitted lines and they facilitate the observation of the onset of diminished-activity increase for control samples and the denaturation process for alcohol sample for $T > 310$ K. In both graphs the *thick* and *thin solid lines* represent fit to the measured data for control and alcohol samples, respectively. *Arrows* indicate the positions of breaks in the two graphs. *Points* and *bars* represent the mean ± error estimate from three experiments

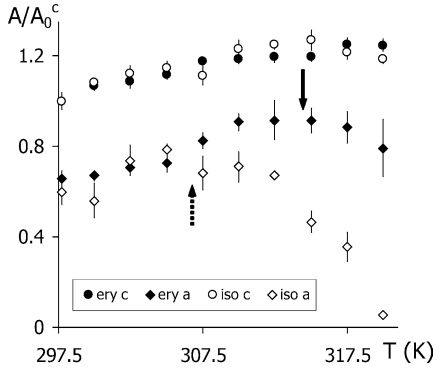

Fig. 4 Comparison of the temperature dependence of the intact erythrocyte AChE activity (*ery*; *filled symbols*) and of the isolated AChE activity (*iso*; *open symbols*) for control samples (*c*; *circles*) and for *n*-butanol samples, 0.22 M (*a*; *diamonds*). The activity values for erythrocyte and isolated AChE were normalized to the value of activity for corresponding control samples at 297.5 K (A_0^c). The temperature at the start of denaturation process for alcohol samples is higher in the case of erythrocyte AChE (*solid arrow*) than isolated AChE (*dashed arrow*). *Points* and *bars* represent mean ± error estimate from one experiment for isolated AChE and from three experiments for intact AChE

Temperature-dependence (Arrhenius) analysis

The temperature-dependence plots of different quantities presented in the Results were examined by linear regression least-squares analysis. The assignation of a break in these plots required that the correlation coefficient above and below the break point was significantly larger than the correlation coefficient for a single line.

Enzyme activity modeling

In order to study the modulation of AChE activity by the changed fluidity of the lipid environment, an appropriate measure of local fluidity had to be chosen. We decided to use the domain-type order parameter S_i, because this spectral parameter has the greatest impact on the goodness of fit within the presented spectrum-simulation model in the EPR spectrum decomposition.

Four general assumptions were used in the AChE activity modeling: (1) Michaelis-Menten kinetics is assumed (Ruano et al. 2000); (2) the Michaelis-Menten constant does not depend on temperature $K_m \neq K_m(T)$ (Spinedi et al. 1988); (3) K_m does not depend on domain type because the membrane domain structure changes with temperature, but the Michaelis-Menten constant does not; and (4) the maximum initial reaction rate $v_{max} = v_{max}(S_i)$ is supposed to depend on the order parameter S_i of the particular domain type i in which enzyme molecules are located, through the influence of ordering on the conformation of the enzyme.

In accordance with the above assumptions, the reaction rate v_i in the particular lipid domain types $i = 1$, 2, 3 can be described as

$$v_i(T, S_i) = \frac{v^i_{max}(T, S_i)}{1 + K_m/c_S} \tag{3}$$

where K_m is the Michaelis-Menten constant, $v_{max}{}^i$ is the maximum initial reaction rate in a particular domain type, and c_S is the substrate concentration. We can write

$$v^i_{max}(T, S_i) = k_i c^i_E = \xi_i Exp[-\Delta G_i(S_i)/RT] N^i_e/(N_A V) \tag{4}$$

where the first two factors on the right-hand side of the equation represent the rate constant k_i, while the remaining factors represent the concentration of enzyme molecules $c_E{}^i$ in domain type i. ξ_i is the frequency factor (simplified to be independent of T), ΔG_i is the activation energy for the enzyme molecule positioned in domain type i (which depends on S_i), R is the gas constant, $N_e{}^i$ is the number of enzyme molecules in domain type i, N_A is Avogadro's number, and V is the sample volume. The overall concentration of enzyme molecules can be expressed as $c_E{}^{total} = N_e{}^{total}/(N_A V)$. From Eqs. (3) and (4) the contribution to the overall activity A of the enzyme molecules in domain type i can be derived

$$\begin{aligned} v_i(T, S_i) &= \frac{1}{1 + K_m/c_S} \xi_i Exp[\Delta G_i(S_i)/RT] c^{total}_E \frac{N^i_e}{N^{total}_e} \\ &= A_i(T\ S_i) \frac{N^i_e}{N^{total}_e} \end{aligned} \tag{5}$$

where A_i corresponds to the local domain-type enzyme activity introduced in Eq. (1).

It is clear from Eqs. (1) and (5) that the overall AChE activity A will be determined by the activities of AChE in particular domain types A_i and their respective weights $N_e{}^i/N_e{}^{total}$. In the following subsections two simple models for the values of $N_e{}^i/N_e{}^{total}$ will be introduced.

Model 1: random distribution of enzyme molecules

If the enzyme molecules are randomly distributed among different domain types (Fig. 1A), then $N^i_e/N^{total}_e = w_i$, where w_i is the proportion of domain type i. Consequently, it follows from Eqs. (1) and (5) that

$$A(T) = \frac{c^{total}_E}{1 + K_m/c_S} \sum_i \xi_i Exp[-\Delta G_i(S_i)/RT] w_i(T) \tag{6}$$

It can then be seen from Eq. (6) that the properties of each domain type should be characterized in terms of the order parameter S_i and proportion w_i in order to determine the overall activity A.

In our case, $A(T)$, $S_i(T)$ and $w_i(T)$ were measured in experiment. Approximate values of ΔG_i can be determined from Arrhenius plots of $A(T)$ as will be explained later, and the values of the constant ξ_i can be fitted with the Gaussian method of least squares so that the difference between the expected values for the activity [right side of Eq. (6)] and the measured values of activity [left side of Eq. (6)] reaches minimum. Below, some

simplifications will be made for ΔG_i and ξ_i, which will be used later in the fitting procedure. Indexes c and a will be utilized to denote control samples and alcohol samples respectively, i.e. samples without *n*-butanol and samples with added *n*-butanol.

The addition of *n*-butanol did not greatly influence the order parameters of the two less-ordered domain types but did influence the order parameter of the most-ordered domain type (Fig. 5). A break in the slope of the temperature dependence of $S_3{}^{a}$ can be seen at the characteristic temperature T^* (Fig. 3A). It approximately holds that $S_i^{c} \approx S_i^{a}$ (Fig. 5) for $i=1$, 2 for the whole studied temperature interval, and for $i = 3$ for the temperatures below T^*. Therefore, based on the supposed influence of ordering on the conformation of the enzyme (on the activation energy), we set $\Delta G_i^{c} = \Delta G_i^{a}$ for $i=1$, 2 for the whole studied temperature interval, and for $i=3$ for the temperatures below T^*. As a consequence of the influence of alcohol molecules on the most-ordered domain above T^*, it will be assumed that $\Delta G_3{}^{a}$ is different below and above T^*.

At this point two additional simplifications were made. Firstly, it was postulated that the enzyme molecules in the less-ordered domain types have the same conformation, so that $\Delta G_2 = \Delta G_1$ (indexes c and a for control samples and alcohol samples were left out; see the discussion above). Secondly, we will assume that the properties of the domain type 3 in *n*-butanol samples become very similar to the ones of 1 and 2 above T^*, as the domain type 3 supposedly becomes more fluid due to the incorporation of *n*-butanol molecules (Arsov et al. 2002). For this reason we set $\Delta G_3{}^{a} = \Delta G_3$ below and $\Delta G_3{}^{a} = \Delta G_1$ above T^* [cf. Eqs. (10) and (11)]. Considering that *n*-butanol is a competitive inhibitor (Curatola et al. 1979; Ruano et al. 2000) so that K_m depends on inhibitor (*n*-butanol) concentration but the maximum initial reaction rate v_{max} does not, and taking into account the above assumptions, Eq. (6) can be suitably rewritten. For samples without alcohol we get:

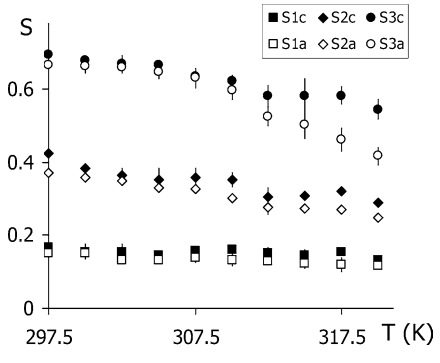

Fig. 5 The temperature dependence of the order parameter S_i for a particular domain type $i=1$, 2, 3, displayed for samples without *n*-butanol (*c*; *filled symbols*) and for samples with added *n*-butanol, concentration 0.22 M (*a*; *open symbols*). *Points* and *bars* represent the mean ± error estimate from three experiments

$$A_1^{c}(T) = A_2^{c}(T) = \frac{c_E^{total}}{1 + K_m^{c}/c_S}\,\xi_1 Exp[-\Delta G_1/RT] \tag{7}$$

$$A_3^{c}(T) = \frac{c_E^{total}}{1 + K_m^{c}/c_S}\,\xi_3 Exp[-\Delta G_3/RT] \tag{8}$$

For alcohol samples we get

$$A_1^{a}(T) = A_2^{a}(T) = \frac{c_E^{total}}{1 + K_m^{a}/c_S}\,\xi_1 Exp[-\Delta G_1/RT] \tag{9}$$

$$A_3^{a,<}(T) = \frac{c_E^{total}}{1+K_m^{a}/c_S}\,\xi_3 Exp[-\Delta G_3/RT], \quad \text{at } T<T^* \tag{10}$$

and

$$A_3^{a,>}(T) = \frac{c_E^{total}}{1+K_m^{a}/c_S}\,\xi_1 Exp[-\Delta G_1/RT], \quad \text{at } T > T^* \tag{11}$$

Because of the continuity, it holds that $A_3{}^{a,<}(T^*) = A_3{}^{a,>}(T^*)$. Then we can derive from Eqs. (10) and (11) that

$$\xi_3 = \xi_1 Exp[-(\Delta G_1 - \Delta G_3)/RT^*] \tag{12}$$

For $T > T^*$ it follows from Eqs. (6), (9) and (11) that

$$A^{a}(T) \propto Exp[-\Delta G_1/RT] \tag{13}$$

so ΔG_1 can be obtained from the Arrhenius plot of A^{a} (Fig. 3B). An estimate for ΔG_3 is obtained from the Arrhenius plot of A^{c} (Fig. 3B). It also follows from Eqs. (6) and (12) that

$$A^{a}(T^*)/A^{c}(T^*) = \frac{1}{1 + K_m^{a}/c_S} \Big/ \frac{1}{1 + K_m^{c}/c_S} \tag{14}$$

The above ratio can be determined from experimental data for $A^{a}(T^*)$ and $A^{c}(T^*)$. When the above estimates are entered into Eqs. (7), (8), (9), (10), (11), and ξ_3 in Eqs. (8) and (10) is substituted with the expression in Eq. (12), only ξ_1 remains to be fitted.

Model 2: enzyme molecules reside in the most-ordered domain type

Within the studied temperature interval all the domain types can be regarded as fluid. However, due to its high order parameter, the most-ordered domain type is expected to represent cholesterol-rich domains. Because the GPI-anchored proteins are found mainly in the lipid domains with special lipid composition (the so-called lipid rafts) that contain a lot of cholesterol (Varma and Mayor 1998; Dietrich et al. 2001), it is expected in the second model that the enzyme molecules reside mainly in domain type $i=3$ (Fig. 1B).

If the enzyme molecules are only in domain type $i=3$, and considering Eqs. (1) and (5), we can derive:

$$A(T) = A_3(T, S_3) = \frac{c_E^{total}}{1 + K_m/c_S}\,\xi_3 Exp[-\Delta G_3(S_3)/RT] \tag{15}$$

In order to find in what way the activation energy ΔG_3 depends on the order parameter of the most-ordered domain type S_3, we have to search for the correlation between activity of AChE and S_3, e.g. the slopes and the positions of breaks (if they are present) in the plots of $\ln(A/A_0)$ vs. $1/T$ and $-S_3$ vs. $1/T$ have to be compared. As will be seen in the Results section, the ratio of these slopes is similar for control samples and *n*-butanol samples, and also the temperatures of the break in the slope of $-S_3{}^{a}$ vs. $1/T$ and the break in the slope of $\ln(A^{a}/A^{a}{}_0)$ vs. $1/T$ are in agreement (within the range of error). Therefore, the value of $\Delta G_3{}^{c,a}/R$ was chosen as an average ratio r of the slopes $\ln(A/A_0)$ vs. $1/T$ and $-S_3$ vs. $1/T$ (Table 1) times the slope for $-S_3$ vs. $1/T$ (Table 2). Equation (15) then becomes

$$A^{c}(T) = \frac{c_E^{total}}{1 + K_m^{c}/c_S}\,\xi_3^{c} Exp\left[-r \cdot \frac{\partial S_3^{c}}{\partial(1/T)}/T\right] \tag{16}$$

for samples with no alcohol added,

$$A^{a,<}(T) = \frac{c_E^{total}}{1 + K_m^{a}/c_S}\,\xi_3^{a,<} Exp\left[-r \cdot \frac{\partial S_3^{a,<}}{\partial(1/T)}/T\right] \tag{17}$$

for alcohol samples below T^*, and

$$A^{a,>}(T) = \frac{c_E^{total}}{1 + K_m^{a}/c_S}\,\xi_3^{a,>} Exp\left[-r \cdot \frac{\partial S_3^{a,>}}{\partial(1/T)}/T\right] \tag{18}$$

for alcohol samples above T^*. The constants of the form $c_E{}^{total}/(1 + K_m/c_S)\xi_3$ in Eqs. (16), (17), and (18) were fitted by the method of least squares so that the difference between the calculated and the measured values of activity was minimized.

Again the continuity $A^{a,<}(T^*) = A^{a,>}(T^*)$ holds so that

$$\xi_3^{a,>} = \xi_3^{a,<} Exp\left[-r \cdot \left(\frac{\partial S_3^{a,<}}{\partial(1/T)} - \frac{\partial S_3^{a,>}}{\partial(1/T)}\right)/T^*\right] \tag{19}$$

Table 1 Ratios[a] of the slopes of $\ln(A/A_0)$ vs. $1/T$ and $-S_3$ vs. $1/T$ for samples without *n*-butanol (*c*) and for samples with added *n*-butanol, 0.22 M (*a*), and calculated weighted mean ratio r for AChE activity modeling according to model 2

	c	a, $T < T^*$	a, $T > T^*$	r
$\frac{\partial \ln(A/A_0)}{\partial(1/T)} \Big/ \frac{\partial(-S_3)}{\partial(1/T)}$	2.2 ± 0.4	4.2 ± 1.4	2.7 ± 0.4	2.5 ± 0.3

[a]Data are presented as values ± SD

Table 2 The slopes[a] of order parameter of the most-ordered domain type $-S_3$ vs. $1/T$ (Fig. 3A) and the slopes of normalized activity $\ln(A/A_0)$ vs. $1/T$ (Fig. 3B) for samples without *n*-butanol (*c*) and for samples with added *n*-butanol, 0.22 M (*a*)

	c	a, $T < T^*$	a, $T > T^*$
$\frac{\partial(-S_3)}{\partial(1/T)}\,(10^{-4} \times K)$	-6.3 ± 0.4	-3.1 ± 0.6	-16 ± 1
$\frac{\partial \ln(A/A_0)}{\partial(1/T)}\,(10^{-4} \times K)$	-14 ± 2	-13 ± 2	-42 ± 3

[a]Data are presented as values of slope ± SE

follows from Eqs. (17) and (18). In order to satisfy this condition the results of fitting will be shown with the average value of $\xi_3{}^{a,>}$ (or $\xi_3{}^{a,<}$):

$$\xi_3^{a,>} \leftarrow \left(\xi_3^{a,>} + \xi_3^{a,<} Exp\left[-r \cdot \left(\frac{\partial S_3^{a,<}}{\partial(1/T)} - \frac{\partial S_3^{a,>}}{\partial(1/T)}\right)/T^*\right]\right)/2 \tag{20}$$

Results

Determination of EPR-spectra parameters for spin-labeled bovine erythrocyte ghosts

The temperature dependence of the domain-type order parameters for control samples S_i^{c} and *n*-butanol samples S_i^{a} is shown in Fig. 5 and the temperature dependence of the proportions for control samples w_i^{c} and *n*-butanol samples w_i^{a} in Fig. 6. There was no significant difference between the values of the order parameters of the two less-ordered domain types, $S_1{}^{c} \approx S_1{}^{a}$ and $S_2{}^{c} \approx S_2{}^{a}$ (Fig. 5). Similar behavior is also seen for the order parameter of the most-ordered domain type below the break-point temperature T^*: $S_3{}^{c} \approx S_3{}^{a}$ for $T < T^*$ (Figs. 3A, 5). Above T^* the $S_3{}^{a}$ value starts to lower more rapidly with temperature than $S_3{}^{c}$: $S_3{}^{a} < S_3{}^{c}$ for $T > T^*$ (Fig. 5). From the plot of $-S_3{}^{a}$ vs. $1/T$ (Fig. 3A), the specific temperature T^* was determined to be $T^* = 306 \pm 1$ K. The effect of addition of *n*-butanol on the order parameter of the most-ordered domain type is seen only above T^*. Consequently, it can be concluded that the incorporation of *n*-butanol molecules into the most-ordered domain type becomes less restricted at T^* (Arsov et al. 2002). The values of slopes of $-S_3$ vs. $1/T$ in Fig. 3A are summarized in Table 2.

It can be seen that the fluidizing effect of alcohol on the membrane is mainly (except for the effect of *n*-butanol on $S_3{}^{a}$ above T^*) realized through the change in proportions when *n*-butanol is added. It can be seen in Fig. 6 that the proportions of the least-ordered domain type are lower in the case of control samples compared to the alcohol samples ($w_1{}^{c} < w_1{}^{a}$), while the opposite situation is seen for the proportions of the most-ordered domain type ($w_3{}^{c} > w_3{}^{a}$). The proportions, w_2, of the domain type with intermediate ordering do not differ much between the control and alcohol samples; the values increase approximately from 0.2 to 0.3 in the studied temperature interval.

Activity measurements

It is important to note that EPR and activity measurements can only be compared if both measurements are performed on the same samples of erythrocyte ghosts.

In Fig. 4 the activities of the intact erythrocyte form and the isolated form of AChE are compared. For temperatures from 297.5–305 K the difference in the

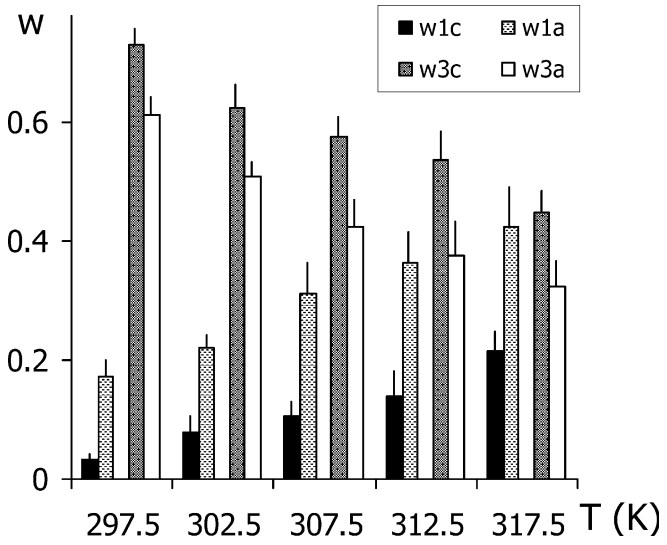

Fig. 6 The temperature dependence of the proportion w_1 of the least-ordered domain-type and the proportion w_3 of the most-ordered domain type of control samples (*c*; *black bars* and *dark grey bars*, respectively), and of *n*-butanol samples, 0.22 M (*a*; *light grey bars* and *white bars*, respectively). The data show the mean ± error estimate from three experiments

activity between the control samples and *n*-butanol samples is comparable for both forms. It is also seen that the temperature at which the denaturation of the enzyme could be detected by the decrease in activity is much lower in the case of the isolated form than in the case of the intact form of the enzyme for *n*-butanol sample (for the control sample, the denaturation does not occur in the studied temperature interval or it starts on its border).

The observed correlation between the temperature dependence of A and S_3 is shown in Fig. 3. As already mentioned, the break in the plot $-S_3{}^a$ vs. $1/T$ appears at $T^* = 306 \pm 1$ K (Fig. 3A). The temperature of the break in the Arrhenius plot of activity of AChE for the *n*-butanol sample $\ln(A^a/A^a{}_0)$ vs. $1/T$ is $T^*{}_A = 305.0 \pm 0.5$ K (Fig. 3B). Therefore, the break temperatures T^* and $T^*{}_A$, respectively, coincide within the range of error. Consequently, the subscript in $T^*{}_A$ will be left out from now on and the notation T^* will be used for both T^* and $T^*{}_A$. In addition to the agreement of break temperatures, it can be seen from the comparison of the two diagrams shown in Fig. 3 that the corresponding slopes have similar ratios (see Table 1). The values of the slopes of $\ln(A/A_0)$ vs. $1/T$ in Fig. 3B are summarized in Table 2. The error-weighted mean ratio of the slopes r is calculated from data in Table 2.

The temperature interval for which the slopes of $\ln(A/A_0)$ vs. $1/T$ were estimated was 297.5–310 K. This interval was chosen because above 310 K the diminished increase in the enzyme activity for control sample (Fig. 3B; Spinedi et al. 1988) and the start of the denaturation process for the alcohol sample (Fig. 3B) appear. The dashed lines in Fig. 3B are extrapolations of the calculated trend lines and are shown in order to facilitate the observation of the correlation between the order parameter of the most-ordered domain type and the AChE activity. For the mentioned reasons, the reduced temperature interval 297.5–310 K will be used for fitting according to the activity models.

The estimates for the activation energies ΔG_3 and ΔG_1 (Table 3) were calculated from the corresponding values of the slopes of $\ln(A^c/A^c{}_0)$ vs. $1/T$ and $\ln(A^a/A^a{}_0)$ vs. $1/T$ (for $T > T^*$), respectively. The value of activation energy for the control sample (11 ± 2 kJ/mol) agrees well with the previously reported values for erythrocyte AChE (Barton et al. 1985, 15 kJ/mol; Spinedi et al. 1988, 12 kJ/mol). Furthermore, the value of the ratio $A^a(T^*)/A^c(T^*)$ [see Eq. (14)], which can be calculated from the measured activity values shown in Fig. 4 or 7, is also shown in Table 3.

Activity modeling

The result of fitting the calculated activity values to the experimentally obtained values according to Eq. (6) (model 1; Fig. 1A) is shown in Fig. 7 (dashed lines). The temperature interval of fitting was 297.5–310 K (for explanation, see previous subsection), but for the sake of comparison with Fig. 3B, the whole measured temperature interval is shown. The points representing the measured activity values for temperatures higher than 310 K are drawn in smaller size. The parameters used in the fitting procedure based on Eqs. (7), (8), (9), (10), (11), (12), (14) are shown in Table 3.

The result of fitting according to Eq. (15) (model 2; Fig. 1B) is also shown in Fig. 7 (solid lines). The value of ΔG needed to fit the calculated activity values to the experimentally obtained values was chosen as the determined ratio r (Table 1) times the corresponding slope for $-S_3$ vs. $1/T$ (Table 2); see Eqs. (16), (17), (18). In addition, Eq. (20) was considered. It can be concluded from Fig. 7 that modeling according to model 2 gives a better fit.

Discussion

The basic step in the study of lipid–protein interaction in membranes is to find the correlation between the dependence of membrane ordering and fluidity on temperature or concentration of a selected compound and the relationships to protein function. In our experiments both disturbances of membrane fluidity were used,

Table 3 Parameters[a] for AChE activity modeling according to model 1

$\frac{1}{1+K^a_m/c_S} / \frac{1}{1+K^c_m/c_S}$	ΔG_3 (kJ/mol)	ΔG_1 (kJ/mol)
0.65 ± 0.02	11 ± 2	35 ± 3

[a]Data are presented as values ± SD

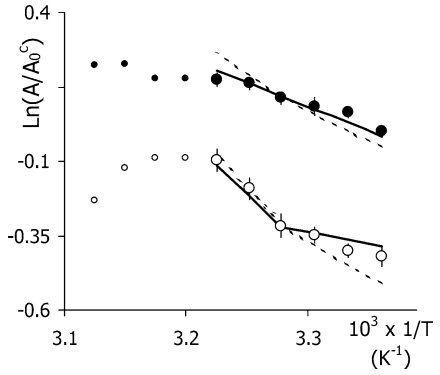

Fig. 7 Modeling the erythrocyte AChE activity according to model 1 (random distribution of enzyme molecules; Fig. 1A) and model 2 (enzyme molecules reside in the most-ordered domain type; Fig. 1B). The modeled activity values are shown as *dashed lines* and *solid lines*, respectively. The measured activity values for control samples (*filled circles*) and *n*-butanol samples (0.22 M; *open circles*) are also shown. The data points of activity measurements are drawn in *smaller size* for temperatures outside the temperature interval of modeling (for $T > 310$ K)

namely temperature as well as *n*-butanol. For this reason, the temperature dependence of the AChE activity combined the direct effect of temperature on the enzyme and the indirect effect of temperature arising through the interaction of *n*-butanol with the lipid environment. This alcohol was used because it has a relatively high buffer membrane partition coefficient compared to its shorter-chained analogues (Seeman 1972).

It is important to note that all the results concerning bovine erythrocyte lateral membrane domain properties determined by the method of EPR-spectrum decomposition are in accordance with the results obtained in previous experiments (Arsov et al. 2002). The addition of alcohol did not influence the temperature dependence of the order parameters of the two less-ordered domain types (Fig. 5). Only a continuous decrease in the lipid ordering with temperature was observed in these two domain types, which means that the acyl-chain conformational and motional freedom is continuously increasing with higher temperatures. In contrast, for the most-ordered domain type ($i = 3$) a break in the slope of the temperature dependence of $S_3{}^a$ can be observed at the characteristic temperature T^* (Figs. 3A, 5). At temperatures below T^*, the influence of alcohol on the membrane fluidity is expressed only in the change of domain-type proportions w_i (Fig. 6), whereas above T^* both the proportions (Fig. 6) and S_3 (Fig. 5) change with the addition of *n*-butanol. The incorporation of *n*-butanol molecules into the most-ordered domain type could become less restricted at T^* as a consequence of the conformational reorganization of the most-ordered domain type (Arsov et al. 2002). It might be expected that the change in the structure of the most-ordered domain type can influence the behavior of the GPI anchor and by that the conformation of a GPI protein (Barboni et al. 1995; Lehto and Sharom 1998). This would then justify the assumption made for *n*-butanol samples that the activation energy of AChE in the most-ordered domain type changes above T^* [compare Eqs. (10) and (11), as well as Eqs. (17) and (18)].

In order to check whether the membrane has any effect on the activity of erythrocyte AChE, the activities of intact and isolated forms of AChE were compared (Fig. 4). The basic difference in the activity between the control samples and *n*-butanol samples is comparable for both forms (before the denaturation process starts). Therefore, this difference seems to be a direct effect of *n*-butanol on AChE activity. On the other hand, the effect of the intact lipid environment is also present. Specifically, the temperature at which denaturation could be detected by activity measurement is much lower for the isolated AChE than the denaturation temperature for intact AChE in alcohol samples. Hence, this might suggest that the membrane has a stabilizing effect on the enzyme (Tsukamoto et al. 1998) and that despite the fact that the AChE catalytic subunit is outside the membrane, AChE still "feels" the membrane.

In the next step, the correlation between the properties of the membrane domain structure and activity of AChE was examined (Fig. 3). The activity values for control samples in Fig. 3B were normalized to the value of activity for the control sample at 297.5 K. Correspondingly, the alcohol samples were normalized to the value of activity for the alcohol sample at 297.5 K. By such normalization the basic difference in the activity between control samples and *n*-butanol samples explained in the previous paragraph was taken into account. Consequently, it is easier to separate the direct effect of temperature on enzyme activity and the change in the activity driven by altered local membrane ordering (the domain-type order parameter). The break temperatures and the ratios of the corresponding slopes of $-S_3$ vs. $1/T$ and $\ln(A/A_0)$ vs. $1/T$ did not differ significantly (Fig. 3). The observed correlation speaks in favor of a possible indirect effect of temperature and *n*-butanol on the AChE activity through their influence on the lipid environment of AChE.

Different methods, e.g. molecular dynamics calculations (Barboni et al. 1995), analysis of differential scanning calorimetry measurements (Reid-Taylor 1999), and fluorescence-resonance energy transfer measurements (Lehto and Sharom 2002), show that the protein moiety of a GPI-anchored protein might be located very close to the lipid bilayer, possibly even touching the membrane (Lehto and Sharom 2002). The contact (constant or occasional) could provide a mechanism for the transfer of structural changes from the membrane to the protein moiety and by that a mechanism of the modulation of the protein function by the lipid bilayer.

Two models for AChE activity dependence on the lateral membrane domain structure were introduced depending on the assumed distribution of enzyme molecules in the membrane. In model 1, random distribution of enzyme molecules in the membrane was assumed (Fig. 1A), and so in addition to the domain-type order parameters, the proportions had to be considered as

well. In model 2, the localization of AChE molecules in the most-ordered domain type was assumed (Fig. 1B) based on the property of GPI-anchored proteins to partition mainly in the cholesterol-rich lipid domains (Varma and Mayor 1998; Dietrich et al. 2001). Therefore, only the behavior of the order parameter of the most-ordered domain type is important for modeling the activity. It can be seen from Fig. 7 that the activity can be fitted more accurately within model 2 (solid lines) than within Model 1 (dashed lines).

At this point, it also has to be mentioned that we did not consider the asymmetry between the exoplasmic and cytoplasmic leaflets in model 1. In general, if a protein is mainly in the exoplasmic leaflet (as is the case for AChE) and is distributed evenly across the leaflet, the proportions in Eq. (6) should be determined for the exoplasmic leaflet only (and not for the whole bilayer). Such determination is possible and was demonstrated by Žuvič-Butorac et al. (1999), but due to unsuitable experimental conditions (low temperature), it could not be applied in our experiments. In the case of model 2, the proportion determination does not cause a problem, since only the behavior of order parameter of the most-ordered domain type (but not the domain-type proportion) is important for modeling the activity.

In conclusion, it was shown that the state of the membrane affects enzyme activity of the GPI-anchored bovine erythrocyte AChE. The comparison of the effects of temperature and *n*-butanol on the activity of the intact erythrocyte and isolated AChE confirmed that the membrane has a stabilizing effect on the enzyme. At the same time, temperature and alcohol also influenced the lateral domain structure of the membrane. This caused a membrane-mediated effect on the erythrocyte AChE activity, which is reflected through the observed correlation between the order parameter of the most-ordered domain type and AChE activity. Furthermore, two models were used to test the correlation between the lateral domain structure of erythrocyte ghost membrane and the AChE activity. In model 1 a random distribution of enzyme molecules in the membrane was assumed, and in model 2 localization of enzyme molecules in the most-ordered domain type was assumed. The results show that model 2 provides a better description of the AChE activity than model 1. Therefore, we believe that AChE molecules are preferentially anchored to specific regions (domains) in the membrane. On the other hand, model 1 might serve as an example of how the domain approach can be applied to proteins distributed between different lateral lipid domains. The presented results provide a new indication that the function of a GPI protein can be modulated by the lipid bilayer. Moreover, the activity seems to be closely linked to the lateral lipid domain structure of the hosting membrane.

Acknowledgements This work was carried out with the financial support of the Ministry of Education, Science and Sport of the Republic of Slovenia.

References

Arsov Z, Schara M, Štrancar J (2002) Quantifying the lateral lipid domain properties in erythrocyte ghost membranes using EPR-spectra decomposition. J Magn Reson 157:52–60

Barboni E, Rivero BP, George AJT, Martin SR, Renouf DV, Hounsell EF, Barber PC, Morris RJ (1995) The glycophosphatidylinositol anchor affects the conformation of Thy-1 protein. J Cell Sci 108:487–497

Barton PL, Futerman AH, Silman I (1985) Arrhenius plot of acetylcholinesterase activity in mammalian erythrocytes and in *Torpedo* electric organ. Biochem J 231:237–240

Bloom M, Thewalt JL (1995) Time and distance scales of membrane domain organization. Mol Membr Biol 12:9–13

Curatola G, Mazzanti L, Lenaz G, Pastuszko A (1979) General anesthetics inhibit erythrocyte acetylcholinesterase only when membrane-bound. Bull Mol Biol Med 4:139–146

Davis PJ, Poznansky MJ (1987) Modulation of 3-hydroxy-3-methylglutaryl-CoA reductase by changes in microsomal cholesterol content or phospholipid composition. Proc Natl Acad Sci USA 84:118–121

Devaux PF (1991) Static and dynamic lipid asymmetry in cell membranes. Biochemistry 30:1163–1173

Dietrich C, Volovyk ZN, Levi M, Thompson NL, Jacobson K (2001) Partitioning of Thy-1, GM1, and cross-linked phospholipid analogs into lipid rafts reconstituted in supported model membrane monolayers. Proc Natl Acad Sci USA 98:10642–10647

Edidin M (1997) Lipid microdomains in cell surface membranes. Curr Opin Struct Biol 7:528–532

Ellman GL, Courtney KD, Andres V Jr, Featherstone RM (1961) A new and rapid colorimetric determination of acetylcholinesterase activity. Biochem Pharmacol 7:88–95

Filipič B, Štrancar J (2001) Tuning EPR spectral parameters with a genetic algorithm. Appl Soft Comput 1:83–90

Freed JH (1976) Theory of slow tumbling ESR spectra for nitroxides. In: Berliner LJ (ed) Spin labeling: theory and applications. Academic Press, New York, pp 53–132

Futerman AH, Low MG, Michaelson DM, Silman I (1985) Solubilization of membrane-bound acetylcholinesterase by a phosphatidylinositol-specific phospholipase C. J Neurochem 45:1487–1494

Gordon LM, Sauerheber RD, Esgate JA, Dipple I, Marchmont RJ, Houslay MD (1980) The increase in bilayer fluidity of rat liver plasma membranes achieved by the local anaesthetic benzyl alcohol affects the activity of intrinsic membrane enzymes. J Biol Chem 255:4519–4527

Hønger T, Jørgensen K, Biltonen RL, Mouritsen OG (1996) Systematic relationship between phospholipase a_2 activity and dynamic lipid bilayer microheterogeneity. Biochemistry 35:9003–9006

Hubbell WL, McConnell HM (1971) Molecular motion in spin-labeled phospholipids and membranes. J Am Chem Soc 93:314–326

Lehto MT, Sharom FJ (1998) Release of the glycosylphosphatidylinositol-anchored enzyme ecto-5'-nucleotidase by phospholipase C: catalytic activation and modulation by the lipid bilayer. Biochem J 332:101–109

Lehto MT, Sharom FJ (2002) Proximity of the protein moiety of a GPI-anchored protein to the membrane surface: a FRET study. Biochemistry 41:8368–8376

Low MG, Saltiel AR (1988) Structural and functional roles of glycosyl-phosphatidylinositol in membranes. Science 239:268–275

Lowry OH, Rosebrough NJ, Farr AL, Randall RJ (1951) Protein measurement with the Folin phenol reagent. J Biol Chem 193:265–275

Marsh D (1981) Electron spin resonance: spin labels. In: Grell E (ed) Membrane spectroscopy. Springer, Berlin New York, pp 51–142

Marsh D (1995) Lipid-protein interactions and heterogeneous lipid distribution in membranes. Mol Membr Biol 12:59–64

Mitchell DC, Lawrence JTR, Litman BJ (1996) Primary alcohols modulate the activation of the G protein-coupled receptor rhodopsin by a lipid-mediated mechanism. J Biol Chem 271:19033–19036

Ogiso T, Iwaki M, Mori K (1981) Fluidity of human erythrocyte membrane and effect of chlorpromazine on fluidity and phase separation of membrane. Biochim Biophys Acta 649:325–335

Reid-Taylor KL, Chu JWK, Sharom FJ (1999) Reconstitution of the glycosylphosphatidylinositol-anchored protein Thy-1: interaction with membrane phospholipids and galactosylceramide. Biochem Cell Biol 77:189–200

Rodgers W, Glaser M (1991) Characterization of lipid domains in erythrocyte membranes. Proc Natl Acad Sci USA 88:1364–1368

Ruano MJ, Sanchez-Martin MM, Alonso JM, Hueso P (2000) Changes of acetylcholinesterase activity in brain areas and liver of sucrose- and ethanol-fed rats. Neurochem Res 25:461–470

Seeman P (1972) The membrane actions of anesthetics and tranquilizers. Pharmacol Rev 24:583–655

Shinitzky M (1984) Membrane fluidity and cellular functions. In: Shinitzky M (ed) Physiology of membrane fluidity, vol 1. CRC Press, Boca Raton, pp 1–51

Silvius JR, Read BD, McElhaney RN (1978) Membrane enzymes: artifacts in Arrhenius plots due to temperature dependence of substrate-binding affinity. Science 199:902–904

Spinedi A, Rufini S, Luly P, Farias RN (1988) The temperature-dependence of human erythrocyte acetylcholinesterase activity is not affected by membrane cholesterol enrichment. Biochem J 255:547–551

Spinedi A, Luly P, Farias RN (1993) Does the fluidity of the lipid environment modulate membrane-bound acetylcholinesterase? Biochem Pharmacol 46:1521–1527

Squier TC, Bigelow DJ, Thomas DD (1988) Lipid fluidity directly modulates the overall protein rotational mobility of the Ca-ATPase in sarcoplasmic reticulum. J Biol Chem 263:9178–9186

Štrancar J, Šentjurc M, Schara M (2000) Fast and accurate characterization of biological membranes by EPR spectral simulations of nitroxides. J Magn Reson 142:254–265

Taguchi R, Ikezawa H (1987) Properties of bovine erythrocyte acetylcholinesterase solubilized by phosphatidylinositol-specific phospholipase C. J Biochem 102:803–811

Tocanne J-F, Cezanne L, Lopez A, Piknova B, Schram V, Tournier J-F, Welby M (1994) Lipid domains and lipid-protein interactions in biological membranes. Chem Phys Lipids 73:139–158

Tomishige M, Kusumi A (1999) Compartmentalization of the erythrocyte membrane by the membrane skeleton: intercompartmental hop diffusion of band 3. Mol Biol Cell 10:2475–2479

Tsukamoto I, Yokono S, Komatsu H, Ogli K (1998) Effects of halothane and supporting membrane lipids on the activity of acetylcholinesterase. Toxicol Lett 100–101:447–450

Varma R, Mayor S (1998) GPI-anchored proteins are organized in submicron domains at the cell surface. Nature 394:798–801

Welti R, Glaser M (1994) Lipid domains in model and biological membranes. Chem Phys Lipids 73:121–137

Yang L, Glaser M (1996) Formation of membrane domains during the activation of protein kinase C. Biochemistry 35:13966–13974

Žuvič-Butorac M, Müller P, Pomorski T, Libera J, Herrmann A, Schara M (1999) Lipid domains in the exoplasmic and cytoplasmic leaflet of the erythrocyte membrane: a spin label approach. Eur Biophys J 28:302–311